Pure Appl. Chem., Vol. 85, No. 7, pp. 1349–1365, 2013.
http://dx.doi.org/10.1351/PAC-CON-12-09-04

Influence of applied pressure on the probability of electronic energy transfer across a molecular dyad*

Mohammed A. H. Alamiry[1], Effat Bahaidarah[1], Anthony Harriman[1,‡], Jean-Hubert Olivier[2], and Raymond Ziessel[2]

[1]Molecular Photonics Laboratory, School of Chemistry, Bedson Building, Newcastle University, Newcastle upon Tyne, NE1 7RU, UK; [2]Laboratoire de Chimie Moléculaire et Spectroscopies Avancées LCOSA, Ecole Européenne de Chimie, Polymères et Matériaux, CNRS, UMR 7515 associé au CNRS, 25 rue Becquerel, 67087 Strasbourg Cedex 02, France

Abstract: A pair of covalently linked molecular dyads is described in which two disparate boron dipyrromethene dyes are separated by a tolane-like spacer. Efficient electronic energy transfer (EET) occurs across the dyad; the mechanism involves important contributions from both Förster-type coulombic interactions and Dexter-type electron exchange processes. The energy acceptor is equipped with long paraffinic chains that favor aggregation at high concentration or at low temperature. The aggregate displays red-shifted absorption and emission spectral profiles, relative to the monomer, such that EET is less efficient because of a weaker overlap integral. The donor unit is insensitive to applied pressure but this is not so for the acceptor, which has extended π-conjugation associated with appended styryl groups. Here, pressure reduces the effective π-conjugation length, leading to a new absorption band at higher energy. With increasing pressure, the overall EET probability falls but this effect is nonlinear and at modest pressure there is only a small recovery of donor fluorescence. This situation likely arises from compensatory phenomena such as restricted rotation and decreased dipole screening by the solvent. However, the probability of EET falls dramatically over the regime where the π-conjugation length is reduced owing to the presumed conformational exchange. It appears that the pressure-induced conformer is a poor energy acceptor.

Keywords: conformation exchange; energy transfer; fluorescence; high pressure; photochemistry; photophysics; spectroscopy.

INTRODUCTION

The efficiency of intramolecular electronic energy transfer (EET), usually expressed in terms of probability or quantum yield to emphasize the fact that the process must compete with other routes for deactivation of the excited state, is a complex function of the local molecular topology [1]. In certain cases, and most often with modified biological media [2], this realization can be used to estimate distances [3], orientations [4], and structural heterogeneity [5] associated with the host medium. Of particular interest are those examples [6] where the molecular conformation changes on a timescale com-

Pure Appl. Chem.* **85, 1257–1513 (2013). A collection of invited papers based on presentations at the XXIVth IUPAC Symposium on Photochemistry, Coimbra, Portugal, 15–20 July 2012.
‡Corresponding author

parable to the EET event because this situation provides unique information about the relative mobility of the surroundings. Such information is crucial for a better understanding of, for example, protein folding [7], vitrification [8], polymer mobility [9] and internal flexibility [10], DNA melting [11], substrate binding [12], and the morphology of conducting polymers [13]. There are numerous constraints associated with how well EET measures molecular topology but the most important feature concerns the clarity with which the transfer mechanism is known. Indeed, three competing mechanisms underpin EET in spatially resolved molecular dyads; namely, through-space Förster (or coulombic) EET [14], through-bond Dexter (or electron exchange) EET [15], and bridge-mediated EET [16], although other mechanisms might contribute at short separations [17]. The key point here is that the various mechanisms each display precise relationships between the rate of ETT and the positioning of the reactants. Thus, uncertainty in the mechanism will result in major complications for interpreting EET probabilities in terms of separation distances and mutual orientations. At short and long separations, or with particular types of linkage between donor and acceptor, it is not too difficult to assert the dominant transfer mechanism. At intermediate separations, loosely defined as being somewhere in the region of 20 Å, the situation is rather unclear and additional input is needed before the transfer mechanism can be resolved in a meaningful manner [18].

It is also recognized that the probability of intramolecular ETT can be affected by changes in temperature [19], solvent polarity [20] or polarizability [21], pH [22], viscosity [23], the presence of adventitious species [24], microporous media [25], templating substrates [26], or cosolvents [27]. In the main, the effects of such perturbations are easily understood but do not help resolve the issue of the relative contribution of particular EET mechanisms. Much less is known about how applied pressure affects the rate of EET in molecular systems, despite the ubiquitous employment of pressure effects in chemistry, biology, and physics. Unlike the innumerable examples of temperature effects, there are in fact very few instances of where pressure can be used to control the likelihood of intramolecular EET in a molecular dyad [28]. This is somewhat surprising because applied pressure can be considered to affect the conformation of the dyad in a logical manner and is a component of many molecular dynamics simulation protocols [29]. Now, very recent work [30] raised the intriguing possibility that applied pressure might be a convenient tool by which to resolve individual Förster and Dexter EET contributions for a donor–acceptor pair separated by ca. 20 Å. This is the only claim to isolate these two mechanisms by direct experimentation and, therefore, the technique deserves further examination. The purpose of this manuscript is to consider how modest pressure influences the efficiency of EET across a fixed-distance molecular dyad dissolved in a fluid solvent at ambient temperature.

BACKGROUND

Although high-pressure techniques have long been applied to spectroscopic investigations in the liquid phase, these have mostly involved infrared [31], Raman [32], NMR [33], and UV–vis absorption [34] spectroscopy. There are very few indications of how pressure affects the probability of EET, and, in fact, research into how pressure might influence the rate of deactivation of an excited state is scant. Early work [35] showed that high pressures help to control the conformation of oligo-phenylene derivatives in solution and thereby exerted a modest influence on the rate of nonradiative decay of the first-excited singlet state. Other work [36] has explored pressure effects on the rotary action of fluorescent molecular rotors in solution. Related studies have addressed how pressure modulates the electron-transfer rates between flexibly linked donor–acceptor pairs [37], notably using metalloporphyrin- and poly(oxometallate)-based reagents, in homogeneous solution. Additional attention has been paid to pressure effects associated with formation of intramolecular excimers [38] and isomerization [39] of cyanine dyes in fluid solution. Several studies [40] have been concerned with the pressure dependence of "twisted charge-transfer state" formation in relatively simple donor–acceptor dyads where viscosity might play a part in controlling internal reorganization of the solute during electron transfer. The effect of solvent friction, discussed in terms of Kramer's theory [41], on the isomerization dynamics of sub-

stituted alkenes has been treated with respect to pressure effects [42]. A common conclusion is that Kramer's theory requires modification before it can be applied to light-induced isomerization processes in liquids.

Research has shown [43] that minor structural perturbations around orthogonal linkages can have profound effects on the dynamics of intramolecular EET for closely spaced reactants. Such findings are of critical importance because they bring into question the validity of Förster-type calculations of EET rates in molecular dyads where the reactant separation is of a comparable magnitude to the sum of the lengths of the transition dipole moment vectors. Recent research [30] has raised the possibility that high pressure can freeze the conformation into the lowest-energy, i.e., the orthogonal, geometry and thereby switch off the through-space contribution to the overall EET process. Of course, this situation demands that the electron-exchange contribution is insensitive to these particular structural changes.

It should be stressed that applied pressure affects both properties of the solvent and the average conformation of the solute and that these changes are difficult to isolate. In particular, high pressure increases the density of the solvent, sometimes inducing an unexpected isomerization [44] that helps to reduce the molar volume, and this affects secondary properties such as the refractive index, dielectric constant, viscosity, solubilization, freezing point, and polarizability. In turn, such pressure-induced perturbations of the solvent properties can affect factors controlling the likelihood of EET. For example, refractive index is important in determining fluorescence quantum yields [45], changes in polarizability will disturb spectral overlap integrals [46], the transition dipole moment vectors might respond to changes in dielectric constant [47], and variations in viscosity could play important roles in bimolecular interactions [48]. These many factors must be considered when searching for the underlying reasons why applied pressure might change the EET probability in certain molecular dyads. In extreme cases, these corrections can be quite severe.

The molecular systems studied herein (Schemes 1 and 2) represent an extension of earlier work where ionic self-association was used [49] to assemble liquid-crystalline materials able to undergo intracomplex EET in both solution and solid phases. Now we examine intramolecular EET across a covalently linked dyad bearing similar chromophoric terminals. The donor is a (yellow) boron tetramethyl-dipyrromethene (Bodipy) dye [50] equipped with the conventional dipyrrin backbone and with an aryl ring at the meso position while the complementary acceptor is also a Bodipy dye but having extended π-conjugation that pushes absorption into the blue region [51]. There is a clear driving force for EET along the molecular axis from yellow to blue dyes. In the context of pressure effects, it is important to note that the blue Bodipy dye bears multiple paraffinic chains that should hinder rotation of this terminal with respect to the molecular axis. In fact, we consider this particular reagent to be fixed in space during the timescale of EET. The yellow donor lacks these fatty chains and is more likely to undergo internal rotation around the connecting spacer unit. To examine the importance of this effect on the EET dynamics, two separate yellow dyes are considered that differ according to the size of the substituents attached to the boron center. These latter groups are selected to influence the rotational diffusional characteristics of the donor.

EXPERIMENTAL

Synthesis and compound characterization

In order to prepare the target dyads **10** and **11** a number of precursors must be synthesized and purified. These were prepared according to Scheme 1 from the starting Bodipy dye **1**. For example, Sonogashira coupling with trimethylsilylacetylene provided dye **2** in 78 % yield. The subsequent Grignard reaction allows replacement of both fluorine atoms with dimethylaminopropyne units, thereby providing dye **3** in 80 % yield. Removal of the silyl-protecting group facilitated isolation of compounds **4** and **6** in excellent yield. These compounds are needed for the preparation of the target dyads (Scheme 2). The extended blue Bodipy dye was prepared from **1** by a Knovenagel reaction involving the gallate alde-

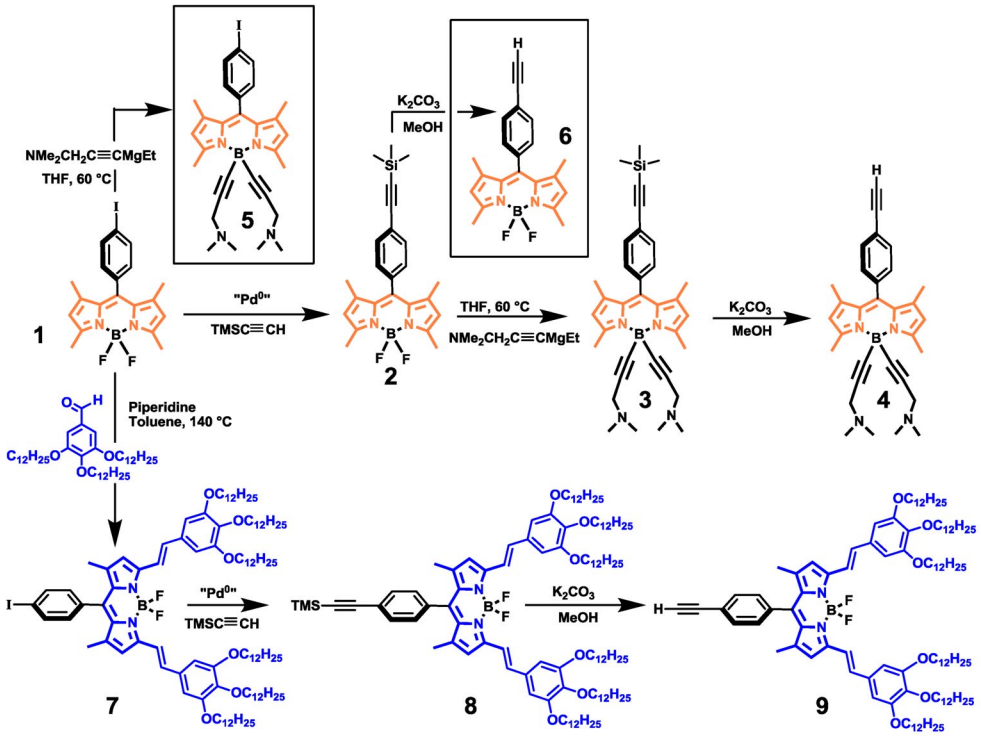

Scheme 1 Molecular formula and compound number for each of the various Bodipy-based precursors used in this study.

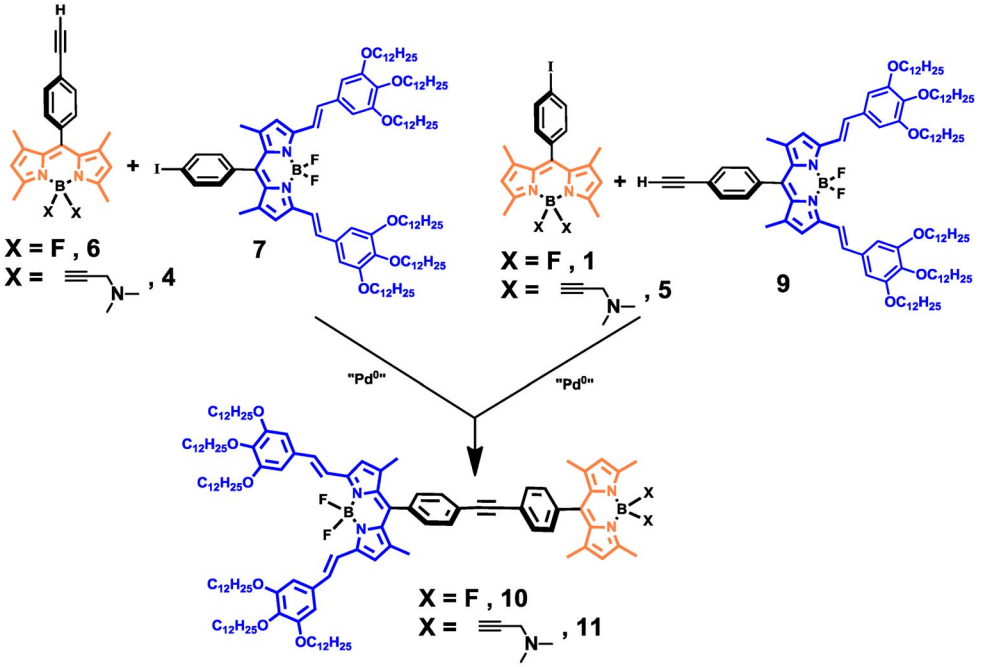

Scheme 2 Synthetic pathways used to access the target molecular dyads **10** and **11**.

hyde under harsh experimental conditions. The blue dye **7** was obtained in 53 %. A sequence of cross-coupling reactions promoted by low valent palladium and subsequent deprotection under basic conditions afforded dye **9** in good yield. Dyes **7** and **9** are required for the synthesis of the main target compounds **10** and **11** (Scheme 2). Two routes for synthesis of these latter materials were devised based on similar protocols developed for somewhat related structures. The first method involves cross-coupling of dyes **4** or **6** with **7** under standard conditions, leading to dyads **10** and **11** (average yields 50 %). The second route is based on a cross-coupling reaction in the reverse sense using the terminal alkyne on the blue dye **9** and the iodo fragment on the tetramethyl-Bodipy frameworks **1** and **5**. Interestingly, this alternative procedure gave more satisfactory yields due to the ease of purification of the final compound (average yields 85 %). The new compounds were purified by column chromatography and characterized by all the usual spectroscopic techniques. Full synthetic details will be published elsewhere.

Spectroscopic investigations

Routine absorption spectral measurements were made with a Hitachi U3310 spectrophotometer while fluorescence spectra were recorded with a Hitachi F4500 spectrophotometer. Solvents for spectroscopic studies were purchased at the highest possible grade and checked for fluorescent impurities before use. Emission quantum yields were measured by standard protocols, using optically dilute solutions, and referenced to appropriate standards. Emission lifetimes were recorded by phase modulation methodology using a temperature-controlled MCP as detector. Emission was collected at 90° to excitation, isolated with a monochromator, and passed to the detector. At least 50 000 counts were accumulated in the peak channel before deconvolution and data analysis. The temporal resolution of this set-up exceeds 15 ps. Temperature dependence studies were made with an Oxford Instruments Optistat DN cryostat. All experiments were repeated several times, and the quoted results are the outcome of signal averaging.

The high-pressure rig was purchased from Stansted Fluid Power Ltd. The general layout comprises a hydraulic compressor constructed from stainless steel. Ethanol is used as the hydraulic medium. The two-stage pump is fitted with an intensifier and diaphragm compressor capable of reaching about 700 MPa. The sample chamber has been machined from a block of stainless steel and is equipped with three optical windows and a Bourdon pressure gauge. The windows show good transmission at wavelengths longer than 370 nm. For absorption measurements, the sample chamber is connected to a Perkin-Elmer lambda-5 spectrophotometer using input and output optical fiber bundles. The absorbance signal is calibrated by reference to the sample solution being recorded in conventional cuvettes with background subtraction. For emission studies, an appropriate laser diode is used as excitation source and output, collected at 90° to excitation, is directed to the spectrofluorimeter with an optical fiber bundle. Purpose-made cells are used to accommodate liquid samples of appropriate concentration. For fluorescence studies, the sample cell is a glass tube, diameter ca. 4 mm, having a narrow mouth that can be capped with a poly(ethylene) seal. The latter takes the form of a short tube that is heat-sealed at one end. For absorption measurements, a hollow glass disk fitted with a narrow inlet tube is used to hold the sample. This disk has a diameter of ca. 1 cm and a pathlength of 2 mm. Again, a poly(ethylene) tube is used as stopper for the cell and the actual pathlength can be calibrated by absorption spectroscopy. Sample cells and poly(ethylene) seals are used once and then discarded.

In a typical experiment, a solution of the relevant compound was prepared in methyltetrahydrofuran (MTHF) and the concentration adjusted appropriately; absorption spectral measurements were made with an absorbance of ca. 0.50 at the peak maximum, and fluorescence studies were carried out with an absorbance of ca. 0.10 at the excitation wavelength. Spectra were recorded under atmospheric pressure and compared with those obtained under conventional conditions using optical cuvettes. The pressure was increased in small jumps, the sample equilibrated at each pressure, and the spectrum recorded. Having reached the maximum pressure, this being restricted to 550 MPa for safety reasons, the pressure was released and spectra recorded to ensure full reversibility of any effects. In other experiments, the pressure was raised to 550 MPa and released slowly with spectra being recorded at each

stage. To check for self-consistency, spectra were recorded at certain pressures after leaving the sample for prolonged periods at that pressure. All measurements were repeated using fresh solutions and, for emission studies, different excitation wavelengths. Data analysis includes making background corrections, especially for absorption measurements, and averaging several spectra recorded under the same conditions.

PHOTOPHYSICAL PROPERTIES OF THE REFERENCE COMPOUNDS

The donor unit used to monitor the effects of pressure on the probability of intramolecular EET in the target dyads is a yellow Bodipy dye of conventional nature (Fig. 1). The photophysical properties of such dyes are well known [52], especially in fluid solution under ambient conditions, and the data collected for **1** and **3** are fully consistent with prior work. Thus, absorption (λ_{max}) and fluorescence (λ_{flu}) maxima, respectively, are found at 500 and 520 nm in MTHF at room temperature (Fig. 2). Replacing the usual fluorine atoms attached to the boron center with alkynylene groups has no obvious effect on these spectral features. For both compounds, the fluorescence quantum yield (Φ_F) recorded in MTHF is ca. 0.72 while the excited-singlet state lifetime (τ_S) is ca. 4.8 ns under the same conditions. The radiative rate constant ($k_{rad} = 1.5 \times 10^8$ s^{-1}) lies within the range found for related Bodipy dyes, as does the Stokes' shift (SS = 600 cm^{-1}). These yellow Bodipy dyes are (photo)stable, highly emissive, monomeric, and readily soluble in common organic solvents.

The acceptor unit is constructed from a bis-styryl Bodipy dye (Fig. 1) where the increased π-conjugation pushes λ_{max} and λ_{flu} to 650 and 675 nm, respectively. It is noticeable that this blue dye, **7**, possesses absorption and emission spectra that are slightly broader than those characterized for the corresponding yellow dyes (Fig. 2), but this is normal for these expanded Bodipy dyes. The Stokes' shift (SS = 570 cm^{-1}) remains closely comparable to that of the yellow dye. but the emission quantum yield ($\Phi_F = 0.54$) is somewhat decreased relative to that of the donor. Both k_{rad} (= 1.3×10^8 s^{-1}) and τ_S (= 4.2 ns) remain in the region found for most Bodipy dyes. The paraffinic chains tend to restrict solubility of the blue dye, at least in a monomeric form, and aggregates tend to form at high concentration, high pressure, or low temperature. These aggregates display characteristic absorption (λ_{max} = 695 nm) and emission (λ_{flu} = 720 nm) spectra with maxima at significantly lower energy than those found for

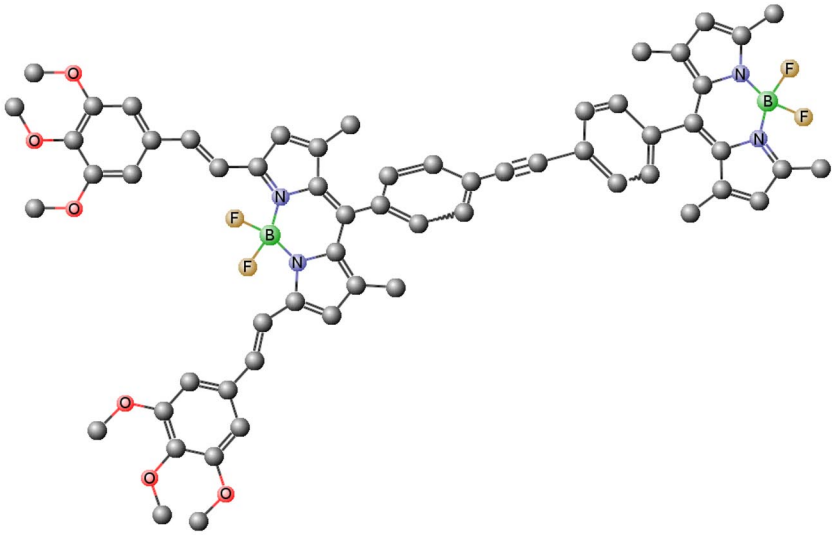

Fig. 1 Energy-minimized molecular conformation computed by TD-DFT for a structural analogue of **10** lacking the paraffinic chains.

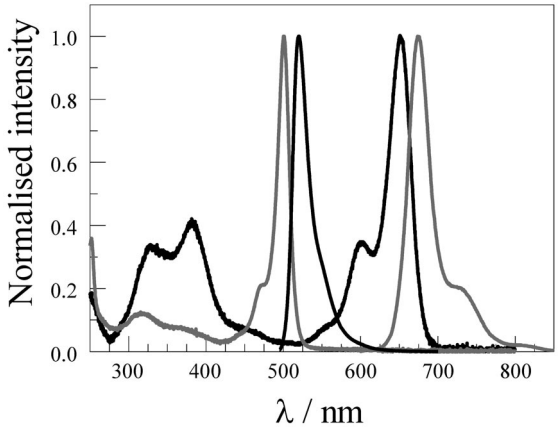

Fig. 2 Normalized absorption and fluorescence spectra recorded for compounds **3** and **7** in MTHF at room temperature, shown as alternate black and gray curves.

the monomer. The spectral properties of the aggregate are reminiscent of those reported [49] recently for liquid-crystalline samples formed by self-association of charged monomers. The former species add to the growing list of fluorescent Bodipy-based aggregates.

Overlap between emission from the yellow donor and absorption by the blue acceptor is modest (Fig. 3), and the energy gap (ΔE_{SS} = 4525 cm^{-1}) between singlet-excited states associated with these two species is sufficiently large for EET to be unidirectional at all accessible temperatures. The spectral overlap integral (J_{DA}) can be calculated from eq. 1 where $\varepsilon(\nu)$ is the molar absorption coefficient for the lowest-energy transition, including all vibrational bands, and $F(\nu)$ is the normalized emission spectral profile. In MTHF at room temperature, J_{DA} has a value of 0.0013 cm. In turn, the transition dipole moments (μ_D or μ_A) can be computed from absorption spectral measurements [53] made for the donor and acceptor in MTHF according to eq. 2. The derived values, again in MTHF at room temperature, are μ_D = 6.70 D and μ_A = 8.06 D, although it has to be stressed that the transition dipole moment vector for the acceptor is considered to be doubly degenerate on the basis of earlier studies [51] made with related push-pull-push Bodipy dyes. The solvent screening factor (s = 0.60) is estimated on the basis of the Onsager cavity [54], as indicated in eq. 3 where n is the solvent refractive index. It is important to note that s is dependent on pressure and temperature because of the induced change in density

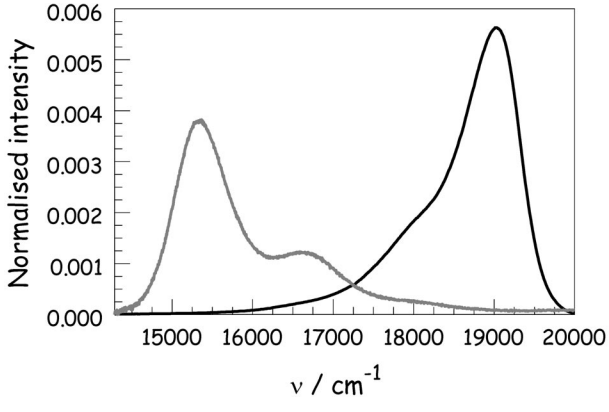

Fig. 3 Illustration of the spectral overlap between donor emission (black curve; compound **3**) and acceptor absorption (gray curve; compound **7**) as recorded in MTHF at room temperature.

of the solvent. The energy-minimized molecular structure deduced for the target dyad lacking the paraffinic chains (Fig. 1) indicates that the boron-to-boron separation distance between yellow and blue dyes is 19.8 Å. This relatively close proximity, taken in conjunction with the combined lengths of the respective transition dipole moment vectors of ca. 17 Å, means that the system falls in the range where the ideal dipole approximation might not hold [55] but where the significance of multipole interactions [56] is expected to be slight. Consequently, we prefer to compute the probability of coulombic EET within the dyad using the Kuhn extended dipole approach [57].

$$J_{DA} = AB\int \frac{f_D(\nu)}{\nu^3}\cdot\frac{\varepsilon_A(\nu)}{\nu}d\nu$$
$$A\int \frac{f_D(\nu)}{\nu^3}d\nu = B\int \frac{\varepsilon_A(\nu)}{\nu}d\nu = 1 \tag{1}$$

$$\frac{\mu_D}{4\pi\varepsilon_0} = \frac{3000\ln 10\hbar c}{8\pi^3 N_A}\cdot\frac{n}{s^2}\int\frac{\varepsilon}{\nu}d\nu \tag{2}$$

$$s = \frac{3}{2n^2+1} \tag{3}$$

Here, the point dipoles inherent to the ideal dipole approximation are replaced by charges assigned to each end of the transition dipole moment vectors. In reality, both the magnitude of the charge ($\pm q_D$ or $\pm q_A$) and their separation length are unknown but they are covered by the basic assumption that $q_D = \mu_D/l_D$, where l_D is taken as the molecular length of the transition dipole (l_D = 7.19 Å; l_A = 9.55 Å) as determined by quantum-chemical calculation. In turn, and allowing for the double degeneracy of the acceptor, the coulombic coupling matrix element (V_{DA}) can be calculated from eq. 4 as the sum of eight electrostatic-style interactions between the respective charges and allowing for their mutual separation (designated as a or b in the equation). In the absence of internal rotation around the connector, and using distances computed for the energy-minimized geometry in the absence of paraffinic chains (Fig. 1), V_{DA} is calculated to be 7.5 cm^{-1}. In fact, rotation of the yellow dye has the effect of reducing V_{DA} and the mean value calculated on the basis of free rotation around the connector is 6.4 cm^{-1}. Finally, the rate constant (k_{XTD}) for coulombic-style EET across the molecular dyad can be calculated from eq. 5 so as to give a mean value of 2.3×10^{10} s^{-1}. This latter value can be compared with the experimental rate constant for EET (k_{EET}) in order to gauge the significance of through-space EET in this system.

$$V_{DA} = q_D q_A\left\{\frac{1}{a_1}+\frac{1}{a_2}+\frac{1}{a_3}+\frac{1}{a_4}-\frac{1}{b_1}-\frac{1}{b_2}-\frac{1}{b_3}-\frac{1}{b_4}\right\} \tag{4}$$

$$k_{EET} = \frac{2\pi}{\hbar}s^2\left|V_{DA}\right|^2 J_{DA} \tag{5}$$

TEMPERATURE-DEPENDENT EMISSION PROPERTIES FOR DYAD 10

Absorption spectra recorded for the two molecular dyads, **10** and **11**, are indistinguishable and display the characteristic features of the yellow and blue terminals (Fig. 4). There is no obvious sign of electronic interaction between the terminals. Excitation of these dyads at wavelengths where only the blue dye absorbs gives rise to the expected fluorescence spectral profile for that dye. For both dyads in MTHF, the derived Φ_F, τ_S, and k_{rad} are in keeping with those recorded for **7** under the same conditions. In marked contrast, excitation at a wavelength where the yellow dye absorbs ca. 77 % of incident photons gives rise to emission from both yellow and blue dyes (Fig. 4). It is notable that when compared

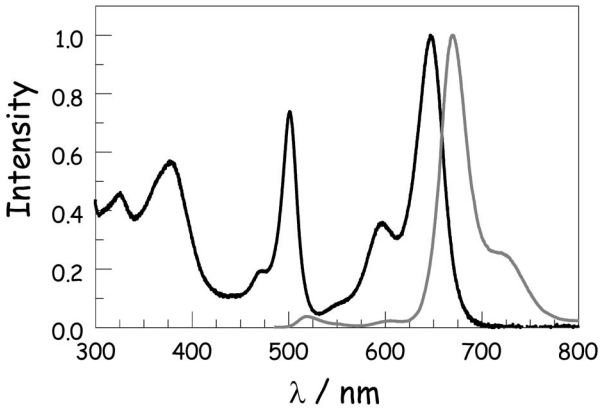

Fig. 4 Normalized absorption (black curve) and fluorescence (gray curve) recorded for the target molecular dyad **10** in MTHF at room temperature. Excitation was made at 490 nm.

to an equimolar mixture of **3** and **7** fluorescence from the yellow dye is heavily quenched while that from the blue dye is enhanced substantially. This situation is fully consistent with efficient EET from yellow to blue dyes, and this was confirmed by excitation spectra. On a quantitative basis, the emission lifetime recorded for the yellow dye in **10** was found to be 29 ± 5 ps, compared to a value of 4.8 ns for the isolated dye **3**. A similar value (τ_S = 32 ± 5 ps) was recorded for the yellow dye present in **11**; here the control dye has an excited-singlet-state lifetime of 4.9 ns. In both molecular dyads, the overwhelming majority of fluorescence attributable to the blue dye grows in after the excitation pulse, as expected for intramolecular EET. For **11**, a small range of dilutions was studied in order to ensure the absence of intermolecular EET under these conditions. From the various lifetime studies, the average rate constant for EET can be estimated as being ca. 3.3×10^{10} s^{-1}. Interestingly, this derived value is reasonably close to that estimated for coulombic EET in this system, such that electron exchange [58] does not appear to play a dominant role in these systems.

On cooling a solution of **10** in MTHF, nothing much happens to the emission spectrum following preferential excitation into either dye until reaching ca. 250 K (Fig. 5). At this temperature, there is a decrease in intensity of emission from the blue dye but without a concomitant increase in fluorescence from the yellow terminal. Thus, there is no change in the probability of EET. As the temperature falls further, quenching of emission from the blue dye becomes more pronounced, and at temperatures around 220 K a new fluorescence band appears with a maximum at ca. 720 nm. This latter band, for which the excitation spectrum shows a maximum at 695 nm, is assigned to an aggregated form of the blue dye. Aggregation is promoted by the presence of the paraffinic chains, a fact ascertained by comparison with other derivatives lacking these substituents. The solvent starts to freeze at about 150 K [59], the glass-transition temperature being around 100 K [60], and at this temperature the emission maximum for the aggregate moves towards 740 nm. In the frozen solvent, there is essentially no emission from the monomeric form of the blue dye. Interestingly, the emission intensity for the yellow dye remains unperturbed, although the spectral profile shows a small blue shift, and there is no recovery of donor fluorescence.

It might be anticipated that high pressure will also promote aggregation of the blue dye but this situation was difficult to confirm experimentally. In most cases, working with a relatively low concentration (i.e., <5 μM) of **10** in MTHF, there was no indication for formation of an aggregate at applied pressures less than 550 MPa. However, in one case with a dyad concentration of ca. 10 μM, the characteristic absorption spectral features of the aggregate appeared at elevated pressure (Fig. 6). Thus, the usual spectrum observed at atmospheric pressure becomes distorted in the region characteristic of the blue dye at pressures above 100 MPa. The absorption band assignable to the aggregate starts to appear

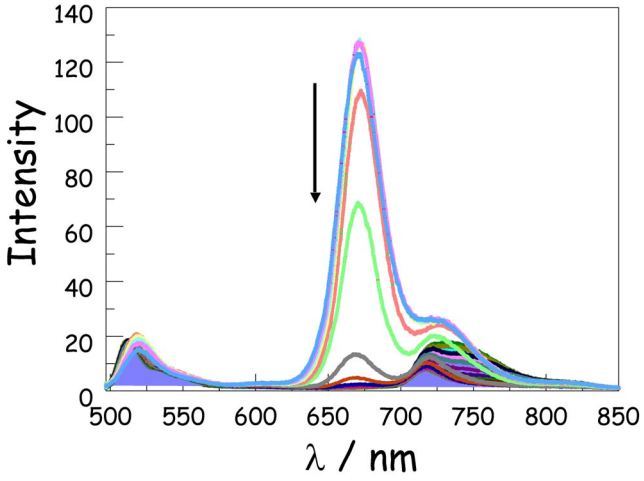

Fig. 5 Effect of temperature on the emission spectral profile recorded for dyad **10** in MTHF: The temperature ranges from 290 to 80 K in increments of 10 K. The excitation wavelength was 490 nm. As the solution cools, emission from the blue dye decreases in intensity and, at low temperature, shifts towards the red.

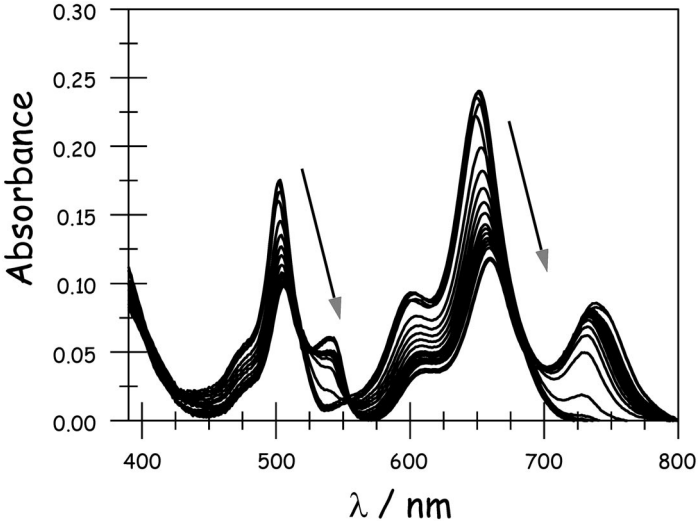

Fig. 6 Effect of applied pressure on the absorption spectral profile recorded for dyad **10** in MTHF: Pressure increases in equal amounts from atmospheric pressure to 550 MPa as indicated by the arrows. N.B.: This experiment corresponds to a relatively high concentration of dye and, in most other cases, aggregation does not occur during the pressure run.

with a maximum at 730 nm but this moves to lower energy with increasing pressure, reaching a wavelength of ca. 740 nm at the highest pressure. Interestingly, the spectra show clear perturbation of the absorption profile due to the yellow dye as the blue dye aggregates. This latter effect helps explain why there is no recovery of emission from the yellow dye during aggregation of the blue counterpart.

PRESSURE DEPENDENCE RECORDED FOR THE REFERENCE COMPOUNDS

Earlier work [30,38] has demonstrated that the photophysical properties of conventional Bodipy dyes, including **1**, in liquid solution are essentially insensitive to changes in applied pressure. Of course, pressure decreases the molar volume of the solvent and thereby raises the solute concentration. In turn, the increased density modifies the polarizability of the solvent and this causes a small red shift for both λ_{max} and λ_{flu}: this latter effect is magnified if the optical transition contains a contribution from charge-transfer interactions since pressure also tends to increase the solvent dielectric constant. For MTHF at 20 °C, the density increases by ca. 20 % at an applied pressure of 550 MPa while the lowest-energy absorption maximum shifts by ca. 5 nm for both **1** and **3**. Over this pressure range, Φ_F increases steadily and reaches a value of 0.77 at the highest pressure (Fig. 7). The origin of this effect can be traced to the pressure-induced increase in refractive index of the solvent. Indeed, the Strickler–Berg expression [61] requires that k_{rad} scales with n^2 and the predicted effect that such a relationship has on Φ_F is included on Fig. 7. It can be concluded, therefore, that applied pressure has little effect on the accompanying rate of nonradiative relaxation of the first-allowed, excited-singlet state of these yellow Bodipy dyes. It should also be noted that release of the applied pressure restores the original properties.

The situation is less clear with extended Bodipy dyes, such as the blue analogue considered here, because of the pendant styryl arms that might twist under applied pressure as a means by which to reduce the molar volume. Now, absorption spectra recorded for **7** in MTHF at room temperature indicate that the absorption maximum moves progressively towards lower energy as the pressure is raised due to the anticipated change in solvent polarizability. There is also an increase in absorbance of ca. 20 % over the full pressure range, which is easily explained in terms of the increased density. At modest pressure, Φ_F increases slightly after due allowance for the change in concentration but this increase is not as high as expected [61] in view of the perturbation of k_{rad} (Fig. 7). As the pressure continues to mount, Φ_F starts to decrease and by 550 MPa has fallen to 0.53 (c.f., Φ_F = 0.54 at atmospheric pressure), whereas the projected value allowing for the change in k_{rad} is 0.61. The implication is that high pressure introduces either an important nonradiative decay route or a change in molecular conformation.

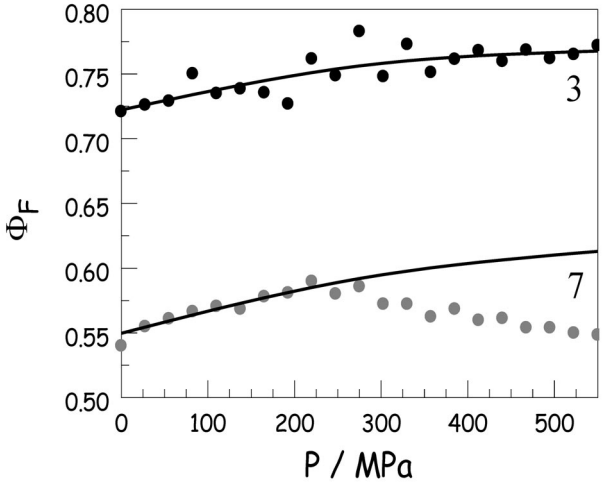

Fig. 7 Effect of applied pressure, *P*, on the fluorescence quantum yields measured for the yellow (**3**) and blue (**7**) control compounds in MTHF at room temperature. The solid lines drawn over the experimental data points correspond to the anticipated pressure-induced effect on Φ_F based entirely on the change in the radiative rate constant (i.e., the change in refractive index of the solvent). The excitation wavelength was 406 nm.

Close examination of the emission spectral profiles recorded for **7** as a function of pressure shows that at ca. 200 MPa a new emission band centered at ca. 620 nm starts to evolve and grows steadily in intensity as the pressure increases (Fig. 8). This is a nonlinear effect (Fig. 8 insert) that is favored at high pressure. Most likely, the effect is caused by structural distortion around one or both styryl arms that serves to decrease the mean π-conjugation length. A similar spectral shift has been reported [51] for push-pull-push Bodipy dyes bearing different appendages attached to the dipyrrin core. Unfortunately, a better assignment of this pressure-induced conformational change must await a more detailed mechanistic examination. For the moment, it is sufficient to accept that this conformational effect is responsible for the decreased Φ_F observed for **7** at elevated pressures.

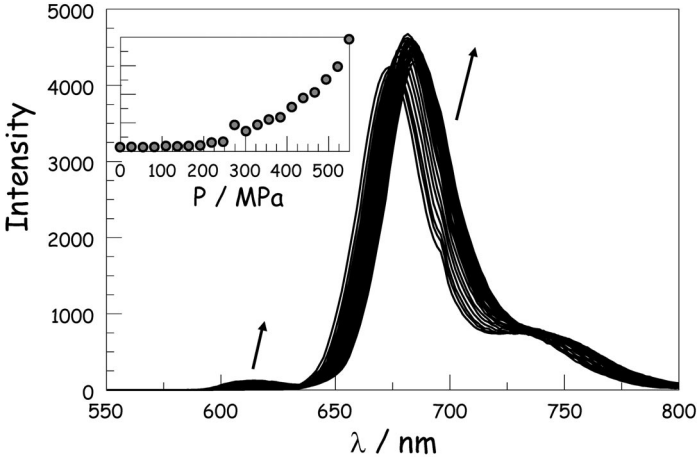

Fig. 8 Effect of applied pressure on the fluorescence spectral profile recorded for the blue control compound **7** in MTHF at room temperature, following excitation at 406 nm. Pressure increases in equal amounts from atmospheric pressure to 550 MPa, as indicated by the arrows. The insert shows the effect of pressure on the integrated emission profile for the new band that appears at around 620 nm.

EFFECT OF PRESSURE ON THE PROBABILITY OF EET FOR THE TARGET DYADS

Under applied pressure, the absorption spectra recorded for dyads **10** and **11** undergo changes similar to those outlined for the respective control compounds. Thus, the absorption maxima for the yellow and blue terminals are clearly evident at 500 and 652 nm, respectively. These maxima move progressively towards lower energy as the pressure is increased (Fig. 9). There is a corresponding increase in absorbance of ca. 20 % over the full pressure range due to compression of the solvent. No other pressure-induced spectral changes are apparent. In both qualitative and quantitative terms, these spectral perturbations are in good accord with expectations based on the control compounds. In particular, there is no sign that either dyad aggregates under these conditions, even after prolonged exposure to high pressure. Furthermore, the changes in band position and intensity are reversed on release of the pressure.

Fluorescence spectra were recorded also for dyads **10** and **11** in MTHF as a function of applied pressure. Various excitation wavelengths were used for these studies. It was noted that direct excitation into the blue dye at $\lambda > 520$ nm gives rise to fluorescence characteristic of that species. Under pressure, there are changes in band position and intensity that closely mirror those observed for **7** in MTHF, including the conformational exchange seen at high pressure (Fig. 10). Adding the second terminal and accompanying connector, therefore, does not affect the sensitivity of the blue dye to changes in either solvent polarizability or density and does not hinder the conformational effect supposed to reduce the

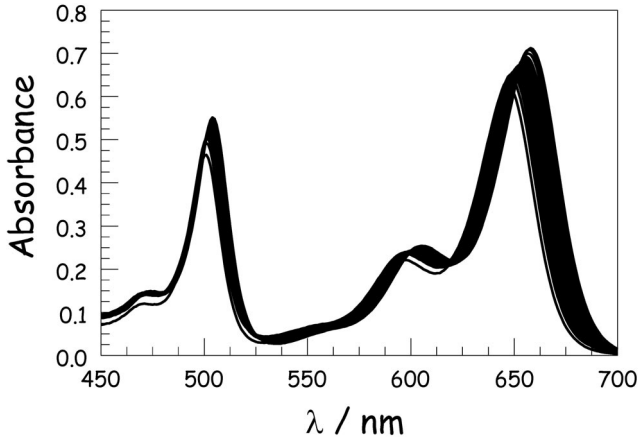

Fig. 9 Effect of applied pressure on the absorption spectral profile recorded for dyad **11** in MTHF at room temperature: Pressure increases in equal increments from atmospheric to 550 MPa.

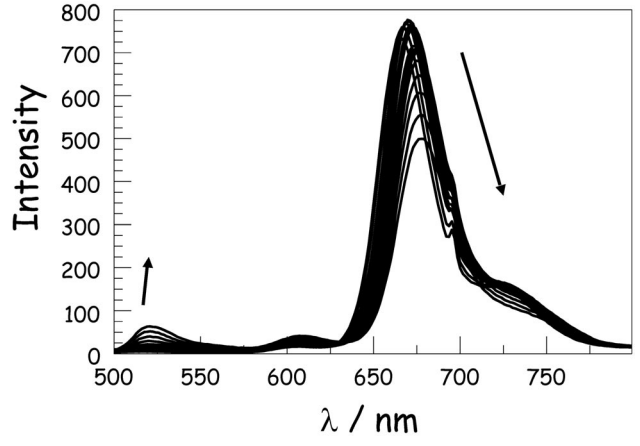

Fig. 10 Effect of applied pressure on the fluorescence spectral profile recorded for dyad **11** in MTHF at room temperature: Pressure increases in equal increments from atmospheric to 550 MPa as indicated by the arrows. Excitation is made at 406 nm.

molecular volume. These studies serve as an invaluable tool by which to calibrate changes in the acceptor emission following excitation into the donor unit.

There is no excitation wavelength at which the yellow dye is the sole absorber, unlike the situation pertinent to the blue dye, and so a variety of wavelengths were used in order to assess the importance of applied pressure on the probability of EET. In all cases, there are two distinct regions of interest in the pressure-emission plots. At modest pressure ($P < 200$ MPa), the emission intensities for both donor and acceptor tend to increase with applied pressure. At higher pressure, however, emission from the acceptor decreases significantly while there is a concomitant increase in fluorescence from the donor. This generic behavior, which holds for both dyads and is independent of excitation wavelength, covers the pressure range where the blue dye undergoes the aforementioned conformational change. Before attempting to rationalize this behavior, several corrections have to be applied to the experimental data. Firstly, the fluorescence signal is isolated spectrally so as to represent the yellow donor or the blue acceptor and the integral corrected for pressure-induced changes in absorbance at the excitation

wavelength. The control dyes were used to indicate the relative absorbance by each dye at that wavelength. Next, the emission yields were corrected for changes in k_{RAD}, as illustrated earlier. The donor signal is now fairly clean, and it is evident that applied pressure causes a nonlinear recovery of donor emission. The signal for the acceptor is distorted by the pressure-induced conformational change, which can be taken into account using a calibration curve constructed following direct excitation into the blue dye. After this critical correction, it is apparent that pressure causes a corresponding decrease in fluorescence from the acceptor. We now consider these "corrected" data (Fig. 11).

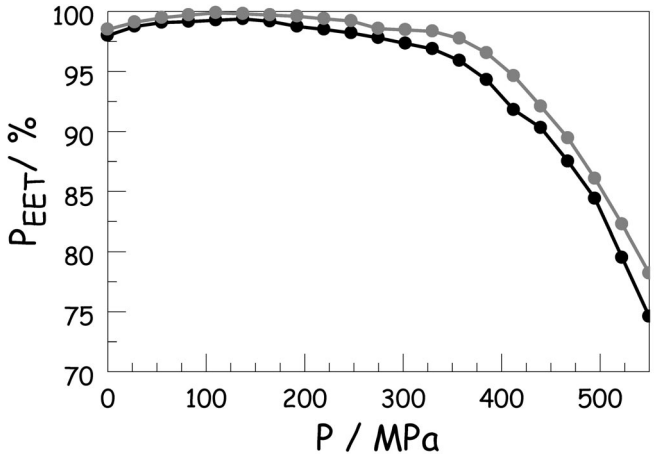

Fig. 11 Effect of applied pressure on the probability of electronic energy transfer (P_{EET}) across the molecular dyad following excitation into the yellow donor. Data given are for dyad **10** (black points) and dyad **11** (gray points) in MTHF at room temperature.

At pressures <200 MPa, the probability (P_{EET}) of intramolecular EET increases slightly with increasing pressure in MTHF at room temperature (Fig. 11). At higher pressure, P_{EET} starts to decrease. In fact, the pressure effect is rather insignificant at low pressure but becomes increasingly more important at pressures above 300 MPa where conformational exchange takes place. The clear indication is that the pressure-induced conformer is a relatively poor energy acceptor. In the low-pressure regime, it might be considered that several pressure-induced phenomena act in a compensatory manner to minimize the effects on P_{EET}. For example, applied pressure is expected to hinder rotation of the donor around the molecular axis and this will increase P_{EET}, at least for the coulombic mechanism. Conversely, applied pressure reduces the magnitude of the dipole-screening factor, s, because of the increase in refractive index. These two effects each cause a 30 % change in the rate of through-space EET over the full pressure range but the effects are opposing. Within experimental limits, the pressure effect in terms of diminishing P_{EET} is roughly the same for the two dyads, although **10** requires slightly less pressure for the conformational change to become noticeable. This might point towards the importance of rotation of the yellow dye. Small changes in the molecular topology are also likely to perturb k_{EET} in this pressure region.

The main effect on P_{EET} is seen at high pressure and corresponds to the conformational change that reduces the effective π-conjugation length. Based on prior work with various synthetic Bodipy dyes [51], the pressure-induced conformer has one styryl arm twisted out of the conjugation path: a crude estimate of the emission maximum for this hypothetical conformer, made by density functional theory (DFT) quantum-chemical calculations, is ca. 565 nm compared to the experimental value of 620 nm. From this, we can infer that the styryl group is only partially unlocked from the dipyrrin core. The most obvious reason for such a pressure-induced change is the need to reduce the molecular volume but this

could also be achieved by compression of the paraffinic chains. In the absence of real information about this structural modification, it is inappropriate to speculate on why the resultant geometry is unfavorable for EET. Conformational change of this type might be expected to induce only a small modification of the rate of electron exchange but would be more significant for Förster-type coulombic interactions. In part, this is because of the change in the nature of the transition dipole moment vector for the acceptor, which would also lose its degeneracy.

CONCLUDING REMARKS

This is the second research article to address how applied pressure might influence the probability of intramolecular EET in a closely spaced molecular dyad. In this case, the direct effect of pressure on P_{EET} is small, perhaps because of compensatory factors, and it appears that the linear topology of the dyad does not facilitate pressure-effect-induced structural modifications. However, at modest applied pressure the acceptor unit distorts in such a way that its electronic properties are perturbed. This leads to a substantial change in color and serves to switch off EET from the attached donor. The process is reversible. It seems reasonable to suppose that such behavior could be exploited to design novel pressure-sensitive materials. To this end, we have started a detailed investigation to examine the pressure-induced conformational exchange undertaken by these extended Bodipy dyes in fluid media.

ACKNOWLEDGMENTS

We thank Newcastle University, Université Louis Pasteur de Strasbourg, EPSRC (EP/E014062/1), and CNRS for providing resources and funding for this work. We are grateful for assistance from Stansted Fluid Power Ltd with setting up the high-pressure rig. E.B. thanks King Abdulaziz University of Saudi Arabia for financial support.

REFERENCES

1. C. Berney, G. Danuser. *Biophys. J.* **84**, 3992 (2003).
2. D. W. Piston, G.-J. Kremers. *Trends Biochem. Sci.* **32**, 407 (2007).
3. A. R. Clapp, I. L. Medintz, J. M. Mauro, B. R. Fisher, M. G. Bawendi, H. Mattoussi. *J. Am. Chem. Soc.* **126**, 301 (2004).
4. B. Schuler, E. A. Lipman, P. J. Steinbach, M. Kumke, W. A. Eaton. *Proc. Natl. Acad. Sci. USA* **102**, 2754 (2005).
5. T. A. Laurence, X. X. Kong, M. Jagger, S. Weiss. *Proc. Natl. Acad. Sci. USA* **102**, 17348 (2005).
6. H. S. Chung, J. M. Louis, W. A. Eaton. *Biophys. J.* **98**, 696 (2010).
7. O. Bieri, J. Wirz, B. Hellrung, M. Schutkowski, M. Drewello, T. Kiefhaber. *Proc. Natl. Acad. Sci. USA* **96**, 9597 (1999).
8. A. Turshatov, J. Adams, D. Johannsmann. *Macromolecules* **41**, 5365 (2008).
9. G. Srinivas, B. Bagchi. *PhysChemComm* **5**, 59 (2002).
10. J. M. Beechem, E. Haas. *Biophys. J.* **55**, 1225 (1989).
11. A. De Cian, L. Guittat, M. Kaiser, B. Sacca, A. Amrane, A. Bourdoncle, P. Alberti, M. P. Teulade-Fichou, L. Lacroix, J. L. Mergny. *Methods* **42**, 183 (2007).
12. C. Y. Zhang, H. C. Yeh, M. T. Kuroki, T. H. Wang. *Nat. Mater*. **4**, 826 (2005).
13. M. K. R. Fischer, T. E. Kaiser, F. Wurther, P. Bauerle. *J. Mater. Chem*. **19**, 1129 (2009).
14. T. Förster. *Naturwissenschaften* **6**, 166 (1946).
15. D. L. Dexter. *J. Chem. Phys*. **21**, 836 (1953).
16. T. Kawatsu, K. Matsuda, J.-Y. Hasegawa. *J. Phys. Chem. A* **115**, 10814 (2011).
17. J. Ray, N. Makri. *J. Phys. Chem. A* **103**, 9417 (1999).
18. C. Curutchet, B. Mennucci, G. D. Scholes, D. Beljonne. *J. Phys. Chem. B* **112**, 3759 (2008).

19. A. C. Benniston, A. Harriman, P. Y. Li, C. A. Sams. *J. Am. Chem. Soc.* **127**, 2553 (2005).
20. S. Jockusch, H.-J. Timpe, W. Schnabel, N. J. Turro. *J. Phys. Chem. A* **101**, 440 (1997).
21. G. W. Robinson. *J. Mol. Spectrosc*. **6**, 58 (1961).
22. T. A. Grusenmeyer, J. Chen, Y. Jin, J. Nguyen, J. R. Rack, R. H. Schmehl. *J. Am. Chem. Soc*. **134**, 7497 (2012).
23. J. Andreasson, A. Kyrychenko, J. Martensson, B. Albinsson. *Photochem. Photobiol. Sci*. **1**, 111 (2002).
24. J. Yu, D. Hu, P. F. Barbara. *Science* **289**, 1327 (2000).
25. S. Chatterjee, S. Nandi, S. C. Bhattacharya. *J. Photochem. Photobiol., A* **173**, 221 (2005).
26. A. M. Brun, A. Harriman. *J. Am. Chem. Soc.* **116**, 10383 (1994).
27. J. Fiedor, M. Pilch, L. Fiedor. *J. Phys. Chem. B* **113**, 12831 (2009).
28. B. Schuler. *Methods Mol. Biol*. **115**, 350 (2007).
29. K. A. Merchant, R. B. Best, J. M. Louis, I. V. Gopich, W. A. Eaton. *Proc. Natl. Acad. Sci. USA* **104**, 1528 (2007).
30. M. A. H. Alamiry, J. P. Hagon, A. Harriman, T. Bura, R. Ziessel. *Chem. Sci*. **3**, 1041 (2012).
31. M. Kato, Y. Taniguchi. *J. Chem. Phys*. **94**, 4440 (1991).
32. R. Sabharwal, Y. Huang, Y. Song. *J. Phys. Chem. B* **111**, 7267 (2007).
33. S. T. Adamy, S. T. Kerrick, J. Jonas. *Z. Phys. Chem. Int. J. Res. Phys. Chem. Chem. Phys.* **184**, 185 (1994).
34. H. Herberhold, S. Marchal, R. Lange, C. H. Scheyhing, R. F. Vogel, R. Winter. *J. Mol. Biol*. **330**, 1153 (2003).
35. S. Webster, D. N. Batchelder. *Polymer* **37**, 4961 (1996).
36. Z. A. Dreger, J. M. Lang, H. G. Drickamer. *Chem. Phys*. **169**, 351 (1993).
37. A. Harriman, K. J. Elliot, M. A. H. Alamiry, L. Le Pleux, M. Severac, Y. Pellegrin, E. Blart, C. Fosse, C. Cannizzo, C. R. Mayer, F. Odobel. *J. Phys. Chem. C* **113**, 5834 (2009).
38. M. A. H. Alamiry, A. C. Benniston, G. Copley, A. Harriman, D. Howgego. *J. Phys. Chem. A* **115**, 12111 (2011).
39. S. Murphy, B. Sauerwein, H. G. Drickamer, G. B. Schuster. *J. Phys. Chem*. **98**, 13476 (1994).
40. A. Zhu, B. Wang, J. O. White, H. G. Drickamer. *J. Phys. Chem. A* **107**, 6932 (2003).
41. J. E. I. Korppi-Tommola, A. Hakkarainen, T. Hukka, J. Subbi. *J. Phys. Chem*. **95**, 8482 (1991).
42. K. Hara. *High Press. Res*. **23**, 225 (2003).
43. M. E. Madjet, F. Muh, T. Renger. *J. Phys. Chem. B* **113**, 12603 (2009).
44. M. A. H. Alamiry, A. C. Benniston, G. Copley, A. Harriman. *RSC Adv.* **2**, 1936 (2012).
45. D. Magde, R. Wong, P. G. Seybold. *Photochem. Photobiol*. **75**, 327 (2002).
46. G. U. Bublitz, S. G. Boxer. *Ann. Rev. Phys. Chem*. **48**, 213 (1997).
47. D. J. Lockhart, S. G. Boxer. *Biochemistry* **26**, 664 (1987).
48. D. R. Crane, P. C. Ford. *J. Am. Chem. Soc*. **113**, 8510 (1991).
49. J.-H. Olivier, J. Barbera, E. Bahaidarah, A. Harriman, R. Ziessel. *J. Am. Chem. Soc*. **134**, 6100 (2012).
50. J.-H. Olivier, J. Widmaier, R. Ziessel. *Chem.—Eur. J.* **17**, 11709 (2011).
51. R. Ziessel, S. Rihn, A. Harriman. *Chem.—Eur. J.* **16**, 11942 (2010).
52. R. Ziessel, A. Harriman. *Chem. Commun*. **47**, 611 (2011).
53. S. Georgakopoulou, R. J. Cogdell, R. van Grondelle, H. van Amerongen. *J. Phys. Chem. B* **107**, 655 (2003).
54. G. D. Scholes, X. J. Jordanides, G. R. Fleming. *J. Phys. Chem. B* **105**, 1640 (2001).
55. K. F. Wong, B. Bagchi, P. J. Rossky. *J. Phys. Chem.* **108**, 5752 (2004).
56. D. L. Andrews. *Phys. Rev. A* **81**, 033825 (2010).
57. V. Czikklely, H. D. Forsterling, H. Kuhn. *Chem. Phys. Lett.* **6**, 207 (1970).
58. A. Harriman, L. J. Mallon, K. J. Elliot, A. Haefele, G. Ulrich, R. Ziessel. *J. Am. Chem. Soc.* **131**, 13375 (2009).

59. A. R. McIntosh, A. Siemiarczuk, J. R. Bolton, M. J. Stillman, T. F. Ho, A. C. Weedon. *J. Am. Chem. Soc.* **105**, 7215 (1983).
60. Q. H. Xu, M. D. Fayer. *J. Chem. Phys.* **117**, 2732 (2002).
61. S. J. Strickler, R. A. Berg. *J. Chem. Phys.* **27**, 814 (1962).

